euspen's 24th International Conference & Exhibition, Dublin, IE, June 2024
www.euspen.eu

Measuring the traction properties of water at high pressures between rolling contacts

Trevor Murphy[1], Alex Slocum[1], Minna Wyttenbach[2] and Jesse Granados[2]

[1]*Department of Mechanical Engineering Precision Engineering Research Group Massachusetts Institute of Technology*
[2]*Department of Mechanical Engineering Massachusetts Institute of Technology*

trmurphy@mit.edu

Abstract

In this work, rolling contacts are designed for evaluating water as a traction drive fluid. In traction drives, lubrication is secondary to providing traction for power transfer between rollers. Roller contacts offer an accessible high-pressure environment for testing. As lubricants often reach a solid-like transition in the contact area, water is hypothesized to undergo a similar transition with the potential to form Ice VI.

In order to study the performance of water as a traction fluid in elements of rolling contact, a system is designed, built, and tested to measure properties as a function of contact stress and relative velocities between rollers. The experimental apparatus takes advantage of commercially available bearing systems. The system was used in static tests and can be further updated for dynamic tests.

Bearing, Design, Evaluation, Experimentation

1. Background and Introduction

In traction drives, lubrication is secondary to providing traction for power transfer between smooth rollers. Traction drive transmissions are like gear drives where the teeth are replaced by smooth rollers that transmit the power through the shearing of a highly pressurized, viscous layer of traction fluid; the high pressure causes traction fluids to become more viscous and approach something similar to a solid like phase transition. With the replacement of teeth by a traction fluid, traction drives offer no backlash, no direct contact in operation, and lower noise [1]. Additionally, the lubricant film protects against wear and damps torsional oscillations [2]. Because power transmission is done by the tractive fluid, having good measurements of friction data is key to the design and modeling of traction drives.

Previous research indicates that, if sufficient pressure is applied, water has the potential to perform comparably to oils as a traction fluid. Water can freeze into ice VI by increasing the pressure to around 1 GPa at room temperature and 0.6 GPa at 0°C [3]. The coefficient of friction of steel on ice I is around 0.24 [4] compared to the about 0.1 of oiled steel systems [2]. Additionally, the limiting shear stress of Ice I is comparable to the limiting shear stress of traction oils ice [5]. Since Ice I has a slightly different structure than Ice VI, the tractive properties of Ice VI with bearing steels is to be studied.

To study tractive properties, there are general guidelines to consider. Traction is considered a system phenomena and consequently testing should be focused on matching the test system with actual application [6] since deviations can lead to tests not matching application observations. [7] says a list of things that can affect the measurement include "material, surface finish, environment, load, velocity of relative motion, nature of relative motion, nature of contact, temperature, sliding history, characteristics of surrounding machine and fixtures" which are influenced by the application and system of interest.

Thus, in this work, a rolling contacts system is designed for evaluating water as a traction fluid. Water is hypothesized to undergo a transition to ice VI within the rolling contacts to then have its tractive properties evaluated. This work focuses on the development of a rotary benchtop test rig to explore the performance of water as traction fluid.

2. Design Process

2.1. Functional Requirements

The main functional requirements for the developed test system involve the measurement of the coefficient of friction (COF) of ice VI in a bearing steel system and flexibility for future developments. The system must create contact pressures large enough to create ice VI (around 1 GPa), measure the COF between the pressurized water and roller, and entrain water in between roller contacts with film thickness larger than the surface roughness of the rollers for full lubrication. The latter is required because if the layer is smaller than the surface roughness, the plates are considered essentially in contact, as lubrication cannot effectively occur at that condition.

The system must also withstand water's corrosive effects for longer than the duration of the experiments. For the initial rendition of the test, the test rig should be benchtop scale for easy build and test, and simple to assemble with few components. Lastly, for future work, the setup should have the capability to facilitate both static and dynamic tests.

2.2. What was built and why

A rotary static friction test apparatus is selected to best match the geometry of roller elements in a traction drive. This setup can initially confirm whether speed is required to entrain water and form a lubrication layer between the roller contacts. Static tests require much fewer components and a simpler design to

start while providing the structural foundation for future dynamic tests.

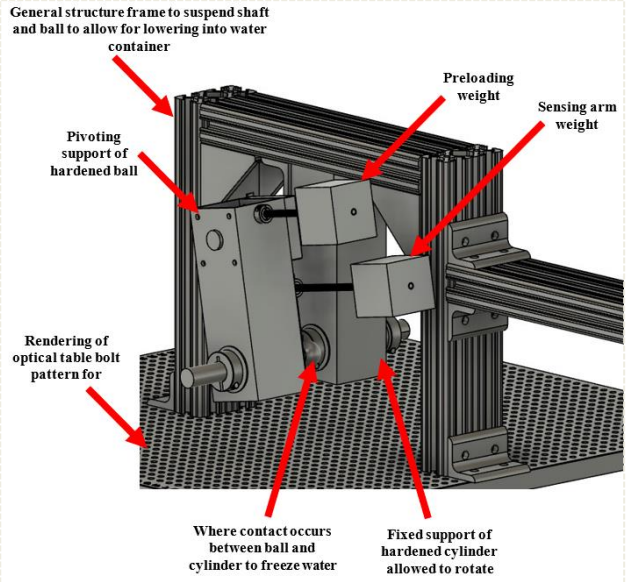

Figure 1. Model of Test Apparatus

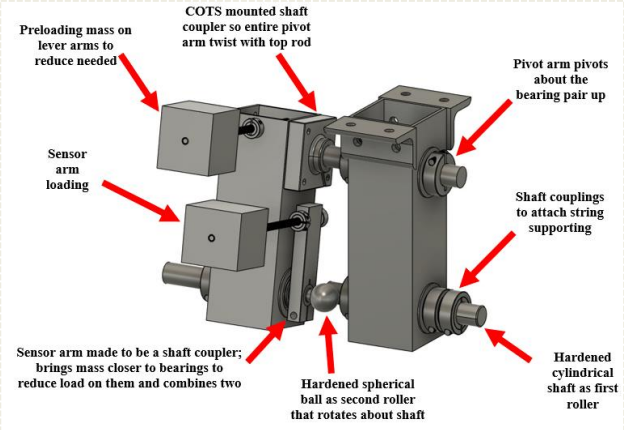

Figure 2. Zoom-in of Test Apparatus Rollers

Figure 1 shows the general concept of the rolling contact system built and tested in this work where **Figure 2** is a zoom-in on the portions that hold the rollers. The rollers consist of a commercial-off-the-shelf (COTS) hardened steel shaft and a tooling ball press fit to be collinear with a second shaft. The nonconformal hertz contact between the sphere and the cylinder allows for smaller, benchtop-sized weights to still reach desired 1 GPa pressures in the contact patch to freeze water due to the very small contact patch area. The sphere is attached to a shaft so that the axis of rotation can be controlled to be the axis of the shaft. Misalignments of the shaft change the radius that the sphere touches at to apply the friction for torque transfer. A 1" sphere and ¾" shaft are selected based on force requirements and Hertz theory scaling:

$$p_m = \frac{2}{3}\left(\frac{6F_{norm}Y_e^2}{\pi^3 R_e^2}\right)^{\frac{1}{3}} \quad (1)$$

In equation (1), p_m is the mean contact pressure set by the pressure needed to freeze the ice, F_{norm} is the normal force on the contact patch, Y_e is the effective Young's modulus of the rollers, and R_e is the effective radius of the rollers.

The supports holding the hardened steel shaft and sphere are oriented vertically in order to submerge as little of the apparatus in water as possible. Additionally, threaded rods are used for precise control over the location of the weights on lever arms providing preload and sensing force. Having the preload and sensing force provided by lever arms about pivots allows for using mechanical advantage to provide desired forces in a configuration that matched the size of the surrounding general structure.

Corrosion-resistant materials such as acetal plastic bearings, hardened stainless steel, and aluminum are selected to address corrosion concerns. COTS ball bearings are used to decrease bearing friction that might confound with the traction properties to be measured.

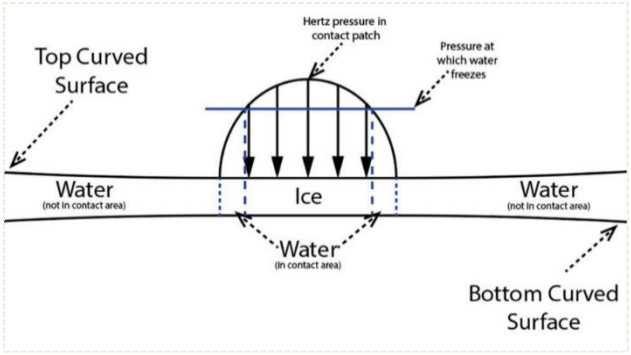

Figure 3. Schematic of Water Freezing in Hertz Contact Patch

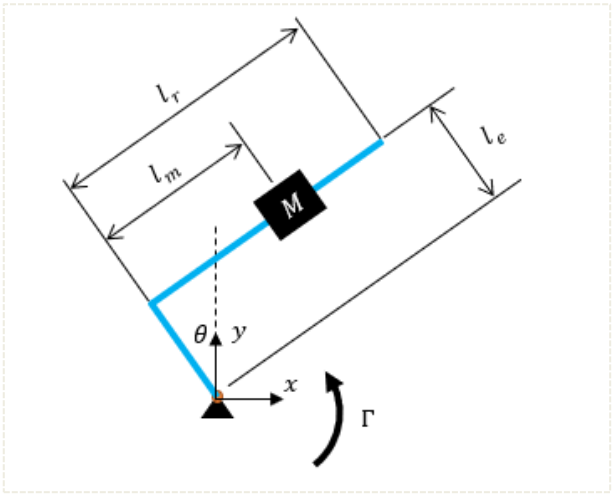

Figure 4. Diagram of Sensing Arm Torque Balance

2.3. How it works

As shown in **Figure 3**, if water is entrained between the rollers, the hypothesis is that ice will form in the center of the contact patch where the hertz pressure reaches and exceeds the freezing pressure, and water will stay liquid elsewhere.

Once ice is presumably formed, the setup is designed to measure the point of slip of the sensing arm, indicating the moment the loading torque overcomes the friction in the system. This angle can be related to a COF of the system from a torque balance applied to the shaft holding the sensor arm with

$$\mu = \frac{\left(-m_e\frac{l_e}{2}\sin\theta + m_r\left(-l_e\sin\theta + \frac{l_r}{2}\cos\theta\right) + M(-l_e\sin\theta + l_m\cos\theta)\right)g}{F_{norm}r_{ball}} \quad (2)$$

where the geometry of the balance is shown **in Figure 4**, m_b, m_e, m_r are the masses of the lengths l_b, l_e, and l_r respectively, F_{norm} is as previously described, r_{ball} is the radius of the ball, M is the mass of the sensing arm weight placed whose center of mass is at l_m, g is the acceleration of gravity, and θ is the angle at which the sensor arm slips completely.

2.4. Testing Conditions

The general test procedure involves resetting the rollers to a position that the sensor arm would not immediately slip, pushing the sensor arm slowly to the point of complete slip and recording the angle at which it happened. This procedure is repeated in different environment conditions (dry, wet, cold) and shaft constraints (fixed, unfixed). The environment conditions of dry, wet, and cold correspond to tests run where the system was dry, placed in room-temperature water, and placed in ice water respectively. The typical temperature of the room was around 20°C and the ice water reached bulk temperature of 5°C during testing. The shaft constraints correspond to whether or not the shaft without the sensor arm was prevented from rolling. Fixed constraint corresponds to the shaft being constrained and unable to rotate with the other shaft during the test. Unfixed corresponds to the shaft being free to rotate with the other shaft during the test.

Throughout the tests the preloading on the rollers is set such that high enough pressures occur for water to freeze at 0°C. One final test condition involves increasing the preload such the freezing would be expected to occur at water temperatures above 9°C and is labelled as "Higher Preload".

3. Data

Figure 5 shows the data collected during the static tests with the ranges set by two standard deviations above and below the mean of ten repeated tests, exceptfor the test condition Cold Fixed. Outliers are ignored. The data is presented in the order that it was taken going left to right. The data includes initially a wet fixed and unfixed condition that was done on a separate day.

Beyond the uncertainty from repeatability shown, there is expected extra uncertainty in the accuracy caused by uncertainty in the angle, mass, and length measurements used to calculate the COF with equation (2). The angle sensor had an uncertainty of 1° corresponding to about 0.01 variation in COF. The mass and length measurement uncertainties could contribute 0.02 and 0.001 variation in the values reported.

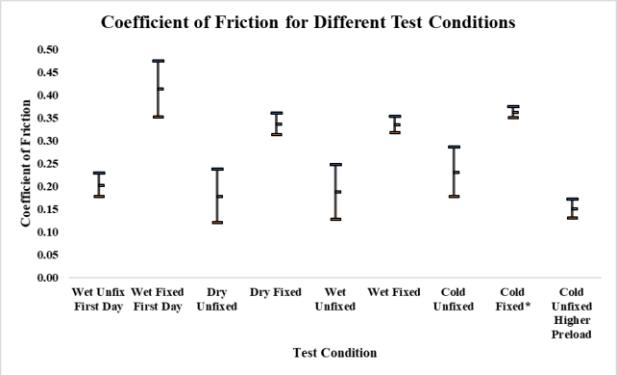

Figure 5. COF Data from 10 Tests in each Condition except Cold Fixed which had only 3 Tests.

4. Discussion

In comparing friction coefficient data, [6][8] recommend using statistical analysis where one of the simplest tests is comparing the ranges of values between data sets where the range is made up of two standard deviations in both directions about the mean. If two ranges overlap, the two sets of data are not statistically different. Following this method of assessment, the majority of unfixed tests are not statistically different despite variation in testing conditions; the majority of fixed tests are not statistically different despite variation in testing conditions; and for the majority of testing conditions, fixed data and unfixed data are statistically different.

Within the fixed condition, the similarity of results despite changing environment suggests that water did not play a role in affecting the COF measurements in the static test. The similarity within unfixed conditions despite changing environment suggests the same.

Water not playing a role in the static tests seems reasonable since water can squeeze out of the contact area faster than it would experience the pressure to freeze, leading to surface contact instead of lubricated contact. As a first order calculation, the liquid evacuation time, defined as the time it takes for the water thickness to decrease from full film lubrication to thinner than the surface roughness of the plates, can be calculated using lubrication equations [9]. These lubrication equations treat the water-filled contact patch area as two flat plates pressed together with some normal force and result in an evacuation time of

$$t_f = \frac{9\mu\pi^2 p_0 R_s R_c}{4Y_e^2 h_0^2} \tag{3}$$

where R_s is the radius of the sphere, R_c is the radius of the cylinder, h_0 is the initial film thickness, and μ is the viscosity of the fluid. The value that this equation predicts is on the order of tens of nanoseconds to tens of microseconds meaning that it takes very little time for water to evacuate from the contact area, resulting in surface contact.

One way to counteract the liquid evacuation is to entrain the water into the contact by having the contacts move in a dynamic test as opposed to a static test. The speed at which to move the roller surfaces can be estimated by applying Poiseuille-Couette flow between two moving plates and finding the speed of the plates that leads to a net inflow of fluid which gives

$$v > \frac{\Delta P h^2}{12a\mu} \tag{4}$$

where v is the speed of the moving plates, ΔP is the pressure change between the edge and center of the contact patch, a is the contact patch size, and h is the film thickness. Alternatively, one could use the elastohydrodynamic film layer thickness fits provided by [9].

The difference between fixed and unfixed configurations is interesting. In the fixed configuration, the shaft roller is prevented from rotating while the ball roller can rotate under the driving force of the sensing arm. Thus, the motion is always pure sliding between the roller surfaces. The unfixed configuration involves the surfaces rolling on each other. It is unclear what the difference between these two conditions implies at the moment.

One thought is that the rolling surfaces produce less friction between them. The question then is why the friction is so large still since rolling frictions are often much smaller than sliding friction values, often around 0.001. Another possibility is that the rolling allows for movement of the elements below what friction could counteract at its maximum. Friction force can be any value below the max limit it can achieve to initiate motion and the friction force measured in the unfixed condition may be this less-than-max value.

Another possibility is slippage between the surfaces during rolling might affect the measured COF. To test this, a separate test was applied to the setup after the friction tests to see if the shafts slipped relative to each other in the unfixed condition. This test was performed by preloading the setup in the dry unfixed condition and manually rotating the shafts various amounts and comparing the output rotation to the rotation expected if there was no slip. The results of that test suggest that there was no relative slippage within the angle sensor's measurement error for the unfixed conditions, ruling out this possibility.

5. Conclusions and Next Steps

A rotary benchtop test rig was designed and built to test the traction properties of ice VI. The static tests suggest that water did not participate in the system friction, possibly since there was no entrainment motion of the rollers to prevent the water evacuating the contact patch before freezing. To get ice VI traction properties, surface motion is needed to entrain the fluid for measurement. The test rig is a good foundation for development of these dynamic tests in the future for assessment of the traction properties of ice VI.

References

[1] "Speed Reducers with Traction Drive Technology," *Designatronics Inc*. [Online]. Available: https://www.sdp-si.com/products/Gearheads-Speed-Reducers/traction-drive.php. [Accessed: 16-Feb-2023].

[2] S. H. Loewenthal and E. V. Zaretsky, "Design of traction drives.," Cleveland, Ohio, 1985.

[3] P. W. Bridgman, "Water, in the Liquid and Five Solid Forms, under Pressure," *Proc. Am. Acad. Arts Sci.*, vol. 47, no. 13, pp. 441–558, Jun. 1912.

[4] N. Nakazawa, T. Terashima, and H. Saeki, "Factors Influencing the Coeffecient of Friction Between Sea Ice and Various Materials," *Proc. Civ. Eng. Ocean*, vol. 8, pp. 141–145, 1992.

[5] H. Saeki, T. Ono, N. E. Zong, and N. Nakazawa, "Experimental Study on Direct Shear Strength of Sea Ice," *Ann. Glaciol.*, vol. 6, pp. 218–221, 1985.

[6] G. E. Totten, *ASM Handbook, Volume 18 - Friction, Lubrication, and Wear Technology (2017 Revision)*. ASM International, 2017.

[7] P. J. Blau, "Appendix: Static and Kinetic Friction Coefficients for Selected Materials," *ASM Handbook, Volume 18 - Friction, Lubrication, and Wear Technology*. ASM International, pp. 70–75, 1992.

[8] K. G. Budinski, "Laboratory Testing Methods for Solid Friction," *ASM Handbook, Volume 18 - Friction, Lubrication, and Wear Technology (2017 Revision)*. ASM International, pp. 44–55, 2017.

[9] B. J. Hamrock, S. R. Schmid, and B. O. Jacobson, "Fundamentals of Fluid Film Lubrication," *Fundam. Fluid Film Lubr.*, 2004.